2018 IEEE International Conference on Robotics and Automation (ICRA)
May 21-25, 2018, Brisbane, Australia

Avoiding Human-Robot Collisions using Haptic Communication

Yuhang Che*, Cuthbert T. Sun*, and Allison M. Okamura

***Abstract*— Fully autonomous navigation in populated environments is still a challenging problem for mobile robots. This paper explores the idea of using active human-robot communication to facilitate navigation tasks. We propose to convey a robot's intent to human users via a wearable haptic interface. The interface can display distinct haptic cues by modulating vibration amplitudes and patterns. We applied the concept to a single human/single robot orthogonal encounter scenario, where one of the two parties has to yield the right of way to avoid collision. Under certain conditions, the robot's intent (to yield to the human or not) is revealed to the human via the haptic interface prior to the interaction. We conducted an experiment with 10 users, in which the robot was teleoperated as a substitute for autonomy. Results show that, when given priority, users become more risk-accepting and use different strategies to navigate the collision scenario than when the robot takes priority or there is no haptic communication channel. In addition, we propose a social-force based model to predict human movement during navigation. The effect of communication can be explained as a shift in the user's safety buffer and expectation of the robot's future velocity.**

I. Introduction

Mobile robots are expected to become common in public spaces and places of work to improve service in terms of accuracy and efficiency. Their applications range from manufacturing and support in factories to house cleaning and social services. We are particularly interested in indoor applications, such as item delivery in buildings and personal assistants. Recent developments in autonomy have given robots the capability to navigate in complex environments. However, there are still significant challenges:

- Human workplaces are usually dynamic and have many moving objects. Navigation in cluttered, constantly changing environments is difficult.
- A robot's movement can sometimes be unintuitive and lead to misunderstanding. Moreover, it is challenging to plan behaviors that respect various social rules.

People often communicate with each other by visual, auditory, and tactile means when navigating in crowded environments, as well as in many other interaction scenarios. Thus, appropriate communication between robots and humans is expected to lead to improved robot performance and user experience.

In this paper, we present a study of robot-human communication in an indoor navigation scenario (Fig. 1). We implemented a simple wearable interface that provides haptic feedback regarding a robot's movement intent to a human walking in the vicinity of the robot. We chose to use haptic feedback because (1) it is immediate and targeted, and (2) users' visual and auditory channels may be already loaded. We conducted the user study with the Turtlebot 2 platform, and demonstrated that users can easily understand the robot's intent via haptic feedback, and make adjustments to their paths accordingly.

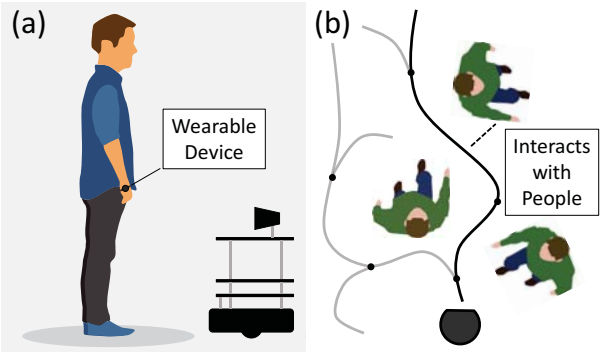

Fig. 1: The concept of an interactive navigation system. (a) The robot can communicate with the user via smart wearable devices. (b) When planning their paths, humans and robots should take potential collisions into consideration.

In addition, we propose a simple predictive model based on the idea of social force in pedestrian navigation [1], [2]. In this model, the interactions between the user and the robot are abstracted as forces that affect the user's movement. We showed that the model can produce reasonable trajectories and capture the main features of the user's movement. However, we emphasize that the model is not meant to accurately predict human movements. The main purpose is rather to explain the effect of communication, and to inform robot planning and decision making in future work.

II. Background

Robot autonomous navigation has been studied for many years. During the past decade, researchers started to shift their effort towards navigation problems in unstructured, populated environments with moving obstacles. Probabilistic methods are often adopted for modeling the environment and planning appropriate actions. Researchers have explored ideas such as Gaussian processes [3], [4], Partially Observable Markov Decision Process (POMDP) [5], and probabilistic velocity obstacles [6]. Besides the traditional planning approaches, bio-inspired algorithms [7], [8] and machine learning techniques [9] also have been studied.

*These authors contributed equally to the work.

This work was supported in part by MediaX at Stanford University and Konica Minolta.

Y. Che and A. M. Okamura are with the Department of Mechanical Engineering, and C. T. Sun is with the Department of Electrical Engineering, Stanford University, Stanford, CA 94305, USA. Email: yuhangc@stanford.edu, csun3@stanford.edu, aokamura@stanford.edu

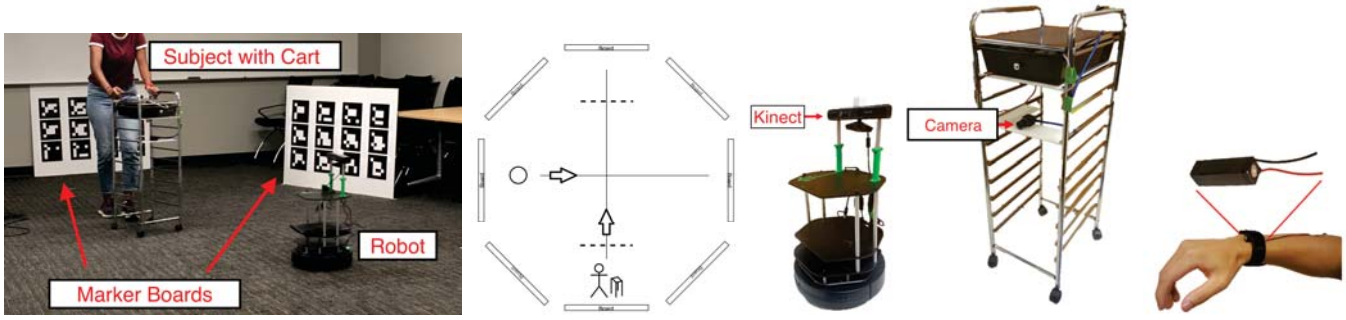

(a) (b) (c) (d) (e)

Fig. 2: Experimental Setup: (a) Experiment field, showing the room and the marker boards. (b) Diagram that shows the experiment task – the human walks between two points, and the robot moves in an orthogonal direction. (c) Turtlebot. (d) User's cart. (e) User wearing the haptic device.

Whether designed to do so or not, when deployed in work and public spaces, robots will have to interact with people in different ways. Many researchers have proposed methods to incorporate interaction into planning frameworks. In [10], [11], the authors developed algorithms that explicitly model human's reaction to a robot (autonomous car), and used it for efficient motion planning and information gathering. The idea to allow robots to act pro-actively is inspiring. However, the algorithm expects the user to be able to infer the robot's intent from its motion. Explicit communication may be more efficient and safer in some scenarios. Another interesting approach for active interaction planning is presented in [12], [13], where the robot can ask for help from humans to overcome its limitations. The authors proposed a planning framework that allows the robot to request help to perform actions that it could not complete otherwise. The work focused on extending the robot's capabilities by interacting with people, while we focus on characterizing the effect of communication on the users' behaviors.

Similar to [10], in [14], [15], the authors presented a proactive navigation approach that takes into account human reactions. The approach made use of a social force model [1] to predict people's reactions to the robot's movement. The social force model was originally developed to study pedestrian dynamics. It abstracts the human as a particle driven by social forces. The force can be produced by other humans in the surroundings, the destination, and other agents like robots. In this paper, we based our approach on [2], where collision prediction is incorporated when calculating social forces. We extend the study in [14] to learn the model parameters under the influence of communication from experimental data.

Although autonomous navigation has been extensively studied, not many works considered direct communication via wearable interfaces. The authors of [16] designed a vibrotactile haptic bracelet for intuitive interaction in human-robot teams. Haptic feedback was used to guide the users to improve human-robot team formation accuracy. The same haptic interface was used in [17] to guide a human user to follow a robot leader. In [18], the authors studied scenarios where a human and a team of robots collaboratively manipulate an object, and haptic feedback was used to inform the user of the states of the robots (in transition vs. stable). To our best knowledge, our work is the first to apply wearable interfaces in human-robot coordination and collision avoidance.

III. Methods

A. Experimental Setup

1) Robot: We used a Turtlebot 2 as the mobile robot platform. Turtlebot 2 is a low-cost, personal robot kit with open-source software. We used a Microsoft Kinect as the 3D sensor, and an ASUS Zenbook UX303UB as the onboard computer to process RGB-D data from the Kinect and to control the robot. All the algorithms described in this and the next section were implemented in Ubuntu 16.04 LTS with the Robot Operating System (ROS Kinetic Kame).

2) Field Setup: The users and robot moved within an empty room, as shown in Figure 2(a). Eight boards (used for tracking, described next) were placed to create a usable space 4.7 m wide by 8.7 m long. The robot moved between the left and right boards, while the user moved between the top and bottom boards, as shown in Figure 2(b). Strips of tape were placed to mark where the human and robot should move. The strips, especially for the human participants, were important because the tracking/recording for each trial was triggered by invisible trip-lines (dotted lines in Figure 2(b)). To elaborate, these horizontal trip-lines were placed at 1.5 m and 6.5 m on the y-axis of the room. Whenever the participant crossed the first line, the trial was initiated, and when the participant crossed the second line, the trial was ended. Further, the haptic communication (if applicable for that trial) was triggered upon the initiation of that trial.

3) Tracking: Existing autonomous mobile robots use a variety of tracking methods to measure the positions of themselves and nearby humans/obstacles. Here we implemented a simple tracking system that fuses visual detection of 2D markers and odometer measurements with the goal creating a robust experimental scenario rather than a practical system for mobile robots. ArUco markers [19] were used in the experiment. Specifically, we constructed "marker boards"

with a grid of 3×4 markers per board, to improve tracking accuracy. A total number of 8 boards were evenly placed around the experiment space to maximize the probability that at least one board can be detected. The poses of the boards were measured from a reference point and kept fixed throughout the experiments. An extended Kalman Filter was used to fuse the visual detection with odometer measurements.

We used the default XBox Kinect camera on the Turtlebot 2 to track the markers, and the robot's odometer to measure its movement. Participants wheeled a cart with a camera mounted at the front, as depicted in Figure 2. This made for a more stable camera image than a body-mounted camera for data collection purposes. The participant's cart was also fitted with an optical flow sensor (PX4FLOW [20]), which acted as an odometer that provides linear and angular velocity measurements. Besides improving the tracking accuracy, the cart was also beneficial because: (a) it simulated a real-world shopping scenario, and (b) it stored all the electronics and the computer required to process the camera images and control the haptic interface.

4) Haptic Device: The haptic interface consisted of a single vibrational motor (Haptuator Mark II), shown in Fig. 2 (e). As introduced in Section I, we used the haptic interface to provide feedback of the robot's intent. The interface is capable of rendering distinct signals by modulating the vibration pattern. In this experiment, we displayed just two haptic cues with different vibration amplitudes and durations. One of the cues was a single long vibration (duration 1.5 sec, max current 250 mA), which represented robot priority (i.e., a warning to the human). The other cue consisted of 3 short pulses (0.2 sec vibration with 0.2 sec pause in between, max current 150 mA), which represented human priority (i.e., encouraging to the human). The idea of robot versus human priority will be explained next. The vibrational motor was controlled by a laptop via a 16-bit analog-to-digital converter. The haptic control loop ran at 1000 Hz.

B. User Study Procedure

A total of 10 people (6 males and 4 females) participated in the experiment after giving informed consent, under a protocol that was approved by the Stanford University Institutional Review Board.

Participants were instructed that their main task would be to walk from one end of the room to the other, and back. There were 3 main scenarios:

1) 12 trials - The participant walks alone
2) 12 training + 24 trials - The participant walks back and forth, while the robot is also moving between two target locations. There is no haptic communication.
3) 12 training + 24 trials - The participant walks back and forth, again with the robot moving between its targets. In this case, there is haptic communication from the robot to the human.

Each trial consisted of the participant walking (with the cart for tracking) from one piece of tape to another on opposite sides of the room. The pieces of tape were placed to provide an end-goal for each trial, and also ensured that the user would walk through the horizontal trip-lines mentioned in the experimental setup. In scenarios involving the robot, the robot would move orthogonally (Figure 2(b)), timed such that there would be a collision scenario with the participant. In these scenarios, either the robot would give the human priority, i.e. the robot would give the human the right of way, and stop/wait for the human to pass; or the robot would give itself priority, i.e. the robot would not yield to the human.

The participants were told that the robot has two main operating modes: one where the participant has priority and the other where the robot gives itself priority. In reality, the robot was teleoperated by the experiment researcher as a substitute of autonomy (a Wizard-of-Oz approach). To properly do so, the teleoperation needed to be performed in a manner that made visual cues unreliable in determining who had priority. This was done with instructions to the teloperator before each run, which both randomized the order of the human/robot priorities and determined the behavior of the robot (how aggressively the robot appeared to move) prior to the collision point. For example, one teleoperation run would have the robot pretend to be passive and tentative, but then give itself priority and ignore the human. Another teleoperation run would have the robot move aggressively towards the collision point, only to stop and wait for the human to pass.

For scenarios 2 and 3, participants were told that they should maintain a constant speed, but they could change their path however they liked to avoid collision with the robot. Also, because each straightaway was treated as a different trial, participants were instructed to wait for the robot to be ready (as determined by the researcher) before proceeding on the next straightaway.

To prevent bias due to participants becoming more familiar with the robot's habits over time during the experiment, the order of scenarios 2 and 3 were flipped for every other participant. Thus, of the ten participants, five did scenario 2 before 3, and five did scenario 3 before 2.

C. Social Force Model with Collision Zone Prediction

We use a social force model as a tool to predict the user's response and analyze the effect of communicating the robot's intent. This model does not reflect all aspects of the user's behavior, and is not accurate for predicting the user's exact trajectory. However, the model can capture important features of user behavior and (as will be shown), its parameters reveal effects of communication. In addition, the model is simple and fast to calculate.

We augmented the social force model originally proposed in [2] with the user's predicted robot velocity and a safety radius, as shown in Figure 3. Instead of the true velocities, we used an "expected" robot velocity $\hat{\mathbf{v}}_r$ in the model. The reasoning is that, when given different feedback information, the user may have a different expectation of the robot's future movement. The expected velocity and the true velocity are

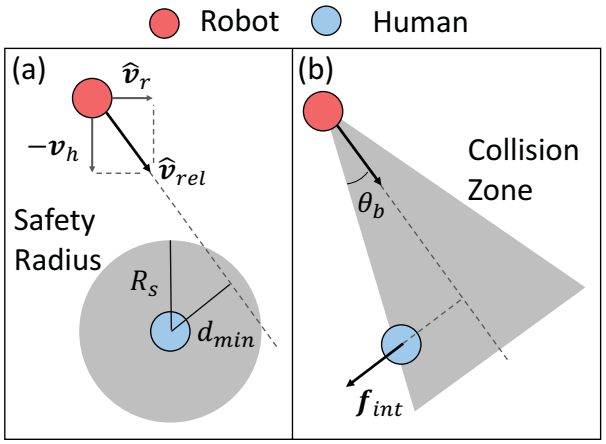

Fig. 3: Social force model with collision zone prediction. (a) The predicted relative velocity and safety radius. $\hat{\mathbf{v}}_r$ is the predicted robot future velocity, $\mathbf{v}_h$ is the human velocity, and $\hat{\mathbf{v}}_{rel}$ is the relative robot velocity. (b) The safety radius criteria can be converted to a collision zone check.

related by:

$$\hat{\mathbf{v}}_r = \mathbf{v}_r + \mathbf{v}_{shift}$$

where $\mathbf{v}_{shift}$ is the shift in user's expectation due to communication. $\mathbf{v}_{shift}$ is assumed to be in the same direction as $\mathbf{v}_r$. The robot's relative velocity is then calculated as $\hat{\mathbf{v}}_{rel} = \hat{\mathbf{v}}_r - \mathbf{v}_h$, where $\mathbf{v}_h$ is the human's velocity. Knowing the direction of the relative velocity, we then project the user's current position onto this line, and obtain the minimum distance d_{min}. If d_{min} is smaller than the user's preferred safety radius, R_s, the social force is then calculated as:

$$|\mathbf{f}_{int}| = A \exp\left(-\frac{d}{B}\right) = A \exp\left(-\frac{|\mathbf{x}_r - \mathbf{x}_h|}{B}\right) \quad (1)$$

with direction perpendicular to $\hat{\mathbf{v}}_r$. Here the parameters A and B determines the maximum magnitude and the decaying rate of the social force. Eq. 1 is equivalent of computing a "collision zone", with the same direction as $\hat{\mathbf{v}}_{rel}$, and a spanning angle $\theta_b = \sin^{-1}(R_s/d)$. If the user's position is within the collision zone, the social force $\mathbf{f}_{int}$ is generated.

To predict the user's future trajectory, we sum over the social forces and calculate the human's acceleration:

$$\ddot{\mathbf{x}}_h = \frac{1}{m}\mathbf{f}_{total} = \frac{1}{m}(\mathbf{f}_{int} + \mathbf{f}_{goal}) \quad (2)$$

Here $\mathbf{f}_{goal}$ is the social force that drives the user to the goal (empirically modeled as $\mathbf{f}_{goal} = k(\mathbf{v}_d - \dot{\mathbf{x}}_h)$), $\mathbf{v}_d$ is the desired velocity that points to the goal directly, and k is a control parameter. We set the mass m to be 1, so that the parameters will not scale with the user's weight.

The parameters A, B, k, $|\mathbf{v}_d|$, R_s, and $|\mathbf{v}_{shift}|$ are learned from experiment data, as explained in Section IV.B. Note that we only need to learn the magnitudes of $\mathbf{v}_d$ and $\mathbf{v}_{shift}$, as their directions are determined by states of the user and the robot at each time step. We will use v_d and v_{shift} to denote their magnitudes in following sections.

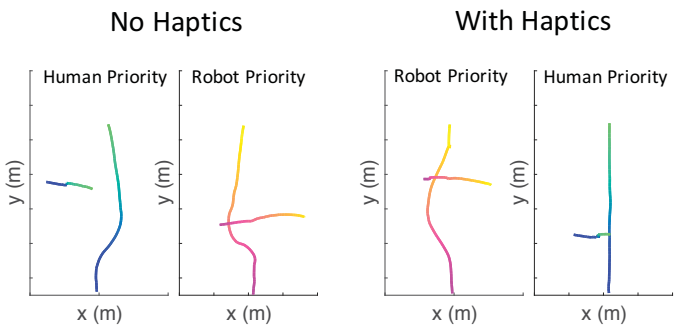

Fig. 4: Example paths/trajectories, where the user is traveling from the bottom to the top, and the robot is traveling from left to right. The two trials on the left side were conducted without haptic communication, so the user did not know when he/she had priority. The two trials on the right side were conducted with haptic communication. (Color gradient represents passage of time, with darker colors indicating earlier times in the trajectory and lighter colors indicating later times in the trajectory.)

IV. Analysis and Results

A. Safety Buffer Distance Metric

The experimental setup allowed us to track the position, velocity, and heading of both the user and the robot for each trial. Figure 4 shows a few sample trials. In the left 2 trials of Figure 4, there was no haptic communication, so the user had to react and maneuver entirely based on visual cues. Thus, their behavior was fairly similar when the user (unknowingly) had priority and when the robot had priority. The teleoperation (Wizard-of-Oz substitution for robot autonomy) was performed in a manner that made it difficult to determine who had priority solely from visual cues. In the right 2 trials of Figure 4, the user received haptic communication about the robot's priority. In the first trial, as soon as robot priority was communicated, the user decided to go behind the robot in order to avoid conflict altogether. This indicates a risk-averse behavior. However, in the second trial, when the user has priority and knows this, the path remains steadfast and straight despite visual cues that suggest an impending collision. This indicates a more risk-accepting behavior.

In an effort to quantify these behavior changes, we defined a metric that we call the "safety buffer" distance, which is inspired by the social force model. The safety buffer distance metric is a measure of the average distance maintained by the user from their future "collision point" throughout a trial:

$$d_s = \frac{1}{T}\sum_{t=0}^{T} d_{min,t} \quad (3)$$

The minimum future distance d_{min} is illustrated in Fig. 3. This point is the closest distance that the robot would be to the user, should they both continue at their respective speeds and directions. However, there is a key difference between the calculation of the safety buffer and the social force – we

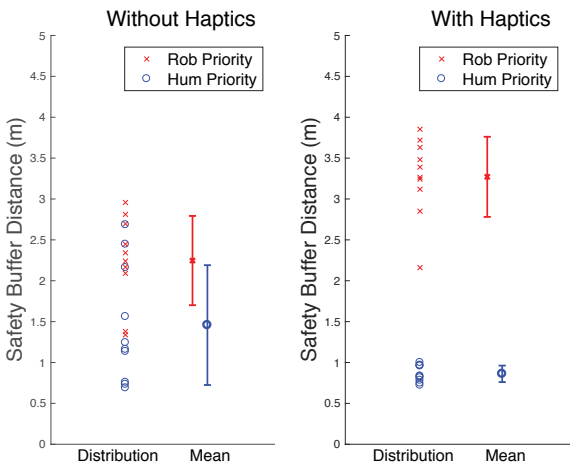

Fig. 5: Individual users and group average/standard deviation of the safety buffer metric (across respective trials) for scenarios 2 (without haptics) and 3 (with haptics). Separation of the clusters for human and robot priority is statistically significant when haptic communication is present.

use the real robot velocity instead of the "expected" robot velocity when calculating the safety buffer: $\mathbf{v}_{rel} = \mathbf{v}_r - \mathbf{v}_h$. This affects d_{min}, which is given by

$$d_{min} = |\mathbf{x}_{rel}| \sin(\theta) = |\mathbf{x}_h - \mathbf{x}_r| \sin(\theta) \tag{4}$$

where $\theta = \cos^{-1}\left(\frac{\mathbf{x}_{rel} \cdot \mathbf{v}_{rel}}{|\mathbf{x}_{rel}||\mathbf{v}_{rel}|}\right)$, is the angle between the relative position and the relative velocity. In some respects, this metric measures how risk averse users are; a larger safety buffer distance means that they have a larger desire to avoid the future collision point.

Additional constraints are placed on d_{min} for practical reasons when calculating the safety buffer distance. First, the safety buffer is only relevant if the participant is close enough to the robot to warrant collision avoiding measures. We observed that the participant would not be affected by the robot if they were far away from each other. A threshold of 3 m is empirically chosen here. Secondly, should the user choose to go "behind" the robot, the safety buffer distance is mathematically infinite, but this prevents calculation of an average safety buffer distance over multiple trials. Thus, a distance of 5 m was set for time steps when this occurs. Finally, once the user passes the robot longitudinally, no more time steps are considered.

The safety buffer metric for each trial was calculated and separated into four main groups: with haptics (human priority + robot priority) and without haptics (human priority + robot priority). Figure 5 plots the average safety buffer (across trials) for each user in each of the four main groups. It then plots the total mean, along with error bars to account for standard deviation across the users. There is a clear and desired separation of the groups when haptics is introduced. This tells us that, indeed, the haptic communication channel was effective and intuitive for the user (i.e. required little thought to properly understand the robot's intent). A one-way ANOVA was run across all users' trials, to test for significant effects of haptics (versus no haptics) and priority (robot versus human) – for a total of four data groups. This is a within-subject ANOVA, where each data point is a separate trial run, collected over all subjects, and separated into one of the four groups. The resulting F-value is F(3, 476) = 165.65, for a p-value $\ll$ 0.0001.Using MATLAB's "multcompare" function and the Bonferroni method, with an α = 0.001 significance level, the result was that all pairwise comparisons were significantly different.

TABLE I: Learned Social Force Parameters

parameter	human priority	robot priority
k (s^{-1})	8.59 $\pm$ 1.41	
A (N)	12.0 $\pm$ 0.2	
B (m)	0.608 $\pm$ 0.094	
R_s (m)	0.178 $\pm$ 0.044	-0.108 $\pm$ 0.015
v_{shift} (m/s)	0.361 $\pm$ 0.047	0.177 $\pm$ 0.045

B. Social Force Model Parameters

To learn the parameters of the social force model from experiment data, we follow a similar procedure to prior work [2]. The overall objective is to minimize a cost function of the form:

$$g(A, B, k, v_d, R_s, v_{shift}) = \frac{1}{NT} \sum_{i=0}^{N} \sum_{t=0}^{T} |\mathbf{x}_{h,i}(t) - \hat{\mathbf{x}}_{h,i}(t)| \tag{5}$$

where T is the total number of time steps, N is the total number of trials of a scenario, and $\hat{\mathbf{x}}_h(t)$ is the predicted position at time t. The prediction is calculated as

$$\hat{\mathbf{x}}_h(t+1) = \hat{\mathbf{x}}_h(t) + \frac{1}{2}(\hat{\mathbf{v}}_h(t) + \hat{\mathbf{v}}_h(t+1))\Delta t \tag{6}$$

$$\hat{\mathbf{v}}_h(t+1) = \hat{\mathbf{v}}_h(t) + \ddot{\mathbf{x}}_h \Delta t \tag{7}$$

Here $\hat{\mathbf{v}}_h$ is the predicted velocity and $\ddot{\mathbf{x}}_h$ is the acceleration calculated from Eq. (2). Here the acceleration is assumed to be piecewise constant. For each participant:

- First, v_d is calculated as the user's average velocity in scenario 1. Then k is learned by optimizing the cost function. Since the robot was not present, the other parameters do not affect the value of g.
- Then, we calculate A, B, and R_s using data in scenario 2, using k and v_d from the first step, and set $v_{shift} = 0$.
- Finally, with A, B, k, and v_d fixed, we obtain the values of R_s and v_{shift} for the positive feedback (human priority) and negative feedback (robot priority), respectively.
- We used Genetic Optimization for all the minimization problems, as suggested by prior works [1], [2].

The learned parameters are summarized in Table I. The values of A, B, and k were kept fixed in the different priority scenarios, and we obtain two sets of R_s and v_{shift} values, one for the human prioritized scenario, and the other for the robot prioritized scenario. The distribution of (R_s, v_{shift}) for all users is shown in Fig. 6. Blue points

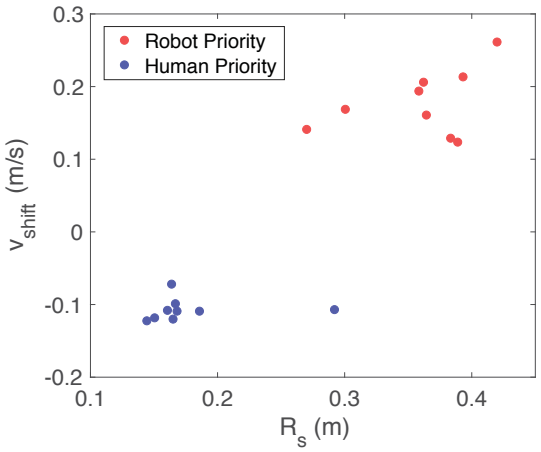

Fig. 6: Distribution of the learned parameters (R_s, v_{shift}) for all users when given feedback. Red points are from trials where the robot prioritized itself, and blue points are from trials where the robot prioritized the user. There is a clear separation of the parameters from the two scenarios.

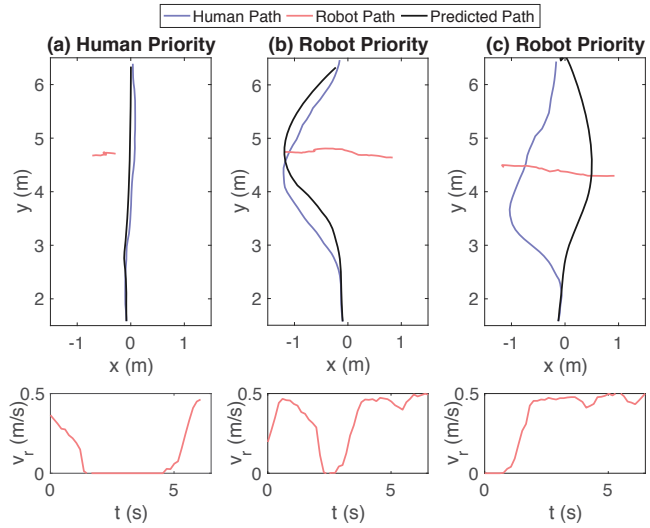

Fig. 7: Examples of predicted user trajectories with learned parameters. First row shows the trajectories. (a) The user had priority. (b) The robot had priority, and the prediction matches the shape of the actual trajectory. (c) The robot had priority, and the prediction does not match the actual trajectory. Second row shows the corresponding robot velocity profiles. Users received feedback in all three trials.

and red points represent the human prioritized and robot prioritized scenarios, respectively. A clear separation of the two distributions can be observed.

While prediction of exact human paths was not a goal of this work, we did wish to predict whether users would pass in front of or behind the robot as an indication of their understanding of priority and use of the feedback. Thus, we used the learned parameters to predict the trajectories of each trial, and compared these with the actual measured trajectories. Three examples are presented in Fig. 7. Figs. 7(a) and 7(b) show successful predictions for different scenarios. Fig. 7(c) demonstrates an incorrect prediction: the actual human trajectory goes behind the robot, while the predicted one goes in front. The robot's velocity profile for these three trials are plotted beneath each set of trajectories. In the incorrect prediction case, the robot initially moved very slowly, leading the model to generate the going-in-front path, which was not actually performed by the user due to awareness of the robot's priority. We calculated the overall percentage of correct predictions, where the model correctly predicts the going-in-front and going-behind behaviors. In the human prioritized scenarios, the model had a success rate of 91%. In the robot prioritized scenarios, the success rate was 83%.

V. Discussion

Figure 5 shows a clear separation of the safety buffer used by participants based on priority when feedback about robot intent is provided. Thus, with haptic communication, the user is more risk averse when told the robot has priority and is more risk accepting when told he/she has priority. This signifies a fundamental shift in user behavior.

The safety buffer metric was designed to describe users' behaviors similarly to the social force model, which explicitly predicts human-robot collisions. Indeed, after fitting social force model parameters, we observed that the key parameters of safety radius and shift of the user's expectation of the robot's velocity vector changed as a result of the haptic communication. This again suggests that the users felt safer and risk accepting knowing that the robot will yield to them. For the shift of users' expected robot velocity, we observe that v_{shift} is generally larger than zero in the robot prioritized trials. This explains the "going behind" behavior; users expected the robot to move aggressively, even if the robot did not do so initially. Similarly, users expected the robot to slow down eventually in the human prioritized trials, and therefore would go in front of the robot, even when the robot was moving aggressively. Conversely, when the robot did not communicate its intent, the users usually acted conservatively and either went behind the robot, or kept a large margin when going in front. Based on these observations, we conclude that users were able to interpret the haptic feedback and the communication improved the efficiency of the human-robot system.

The setup and analysis presented in this paper have several limitations. First, we used a simple haptic interface that can only render discrete vibrational cues. In addition, the device is wired and a laptop is required to control it. In future work, we plan to make wearable haptic interfaces that are wireless and can provide directional cues. Second, the social force model is not very accurate in predicting the details of human movement. As shown in Fig. 7(b), although the predicted shape matches the actual shape of the user's trajectory, there is an offset. As a next step, we plan to develop a model that generates more accurate predictions, and conduct experiments with richer interaction scenarios (e.g. multiple users and robots) to validate the model. Possible

improvements include using nonholonomic model for human movement [21], and using inverse reinforcement learning methods to recover the underlying cost function [9].

VI. Conclusion

In this paper, we presented a study of human-robot communication in a potential collision scenario. The robot can communicate its intent to the user via a haptic interface worn by the user. Results showed that users chose different strategies when receiving different feedback cues about robot versus human priority, and that this communication improved human-robot system efficiency. In addition, we proposed a social force model for the prediction of users' movement. We demonstrated that, with parameters learned from experiment data, the model can predict reasonable trajectories. The shift of model parameters in different scenarios suggests that the users changed their risk acceptance levels and expectation of the robot's behavior when given feedback about priority.

To extend this research, we aim to improve the model and develop planning algorithms that enable the robot to interact with people to improve system performance and efficiency, and well as user experience.

References

[1] D. Helbing and P. Molnar, "Social force model for pedestrian dynamics," *Physical Review E*, vol. 51, no. 5, p. 4282, 1995.

[2] F. Zanlungo, T. Ikeda, and T. Kanda, "Social force model with explicit collision prediction," *Europhysics Letters*, vol. 93, no. 6, p. 68005, 2011.

[3] C. Fulgenzi, C. Tay, A. Spalanzani, and C. Laugier, "Probabilistic navigation in dynamic environment using rapidly-exploring random trees and gaussian processes," in *IEEE/RSJ International Conference on Intelligent Robots and Systems*, 2008, pp. 1056–1062.

[4] P. Trautman, J. Ma, R. M. Murray, and A. Krause, "Robot navigation in dense human crowds: the case for cooperation," in *IEEE International Conference on Robotics and Automation*, 2013, pp. 2153–2160.

[5] A. F. Foka and P. E. Trahanias, "Probabilistic autonomous robot navigation in dynamic environments with human motion prediction," *International Journal of Social Robotics*, vol. 2, no. 1, pp. 79–94, 2010.

[6] C. Fulgenzi, A. Spalanzani, and C. Laugier, "Dynamic obstacle avoidance in uncertain environment combining pvos and occupancy grid," in *IEEE International Conference on Robotics and Automation*, 2007, pp. 1610–1616.

[7] M. P. Garcia, O. Montiel, O. Castillo, R. Sepúlveda, and P. Melin, "Path planning for autonomous mobile robot navigation with ant colony optimization and fuzzy cost function evaluation," *Applied Soft Computing*, vol. 9, no. 3, pp. 1102–1110, 2009.

[8] H. Teimoori and A. V. Savkin, "A biologically inspired method for robot navigation in a cluttered environment," *Robotica*, vol. 28, no. 5, pp. 637–648, 2010.

[9] H. Kretzschmar, M. Spies, C. Sprunk, and W. Burgard, "Socially compliant mobile robot navigation via inverse reinforcement learning," *The International Journal of Robotics Research*, vol. 35, no. 11, pp. 1289–1307, 2016.

[10] D. Sadigh, S. Sastry, S. A. Seshia, and A. D. Dragan, "Planning for autonomous cars that leverage effects on human actions," in *Robotics: Science and Systems*, 2016, DOI:10.15607/RSS.2016.XII.029.

[11] D. Sadigh, S. S. Sastry, S. A. Seshia, and A. Dragan, "Information gathering actions over human internal state," in *IEEE/RSJ International Conference on Intelligent Robots and Systems*, 2016, pp. 66–73.

[12] S. Rosenthal, M. Veloso, and A. K. Dey, "Task behavior and interaction planning for a mobile service robot that occasionally requires help," in *Proceedings of the 9th AAAI Conference on Automated Action Planning for Autonomous Mobile Robots*, 2011, pp. 14–19.

[13] S. Rosenthal and M. M. Veloso, "Mobile robot planning to seek help with spatially-situated tasks." in *AAAI*, vol. 4, no. 5.3, 2012, p. 1.

[14] G. Ferrer, A. Garrell, and A. Sanfeliu, "Robot companion: A social-force based approach with human awareness-navigation in crowded environments," in *IEEE/RSJ International Conference on Intelligent Robots and Systems*, 2013, pp. 1688–1694.

[15] G. Ferrer and A. Sanfeliu, "Proactive kinodynamic planning using the extended social force model and human motion prediction in urban environments," in *IEEE/RSJ International Conference on Intelligent Robots and Systems*, 2014, pp. 1730–1735.

[16] S. Scheggi, F. Morbidi, and D. Prattichizzo, "Human-robot formation control via visual and vibrotactile haptic feedback," *IEEE Transactions on Haptics*, vol. 7, no. 4, pp. 499–511, 2014.

[17] S. Scheggi, M. Aggravi, and D. Prattichizzo, "Cooperative navigation for mixed human–robot teams using haptic feedback," *IEEE Transactions on Human-Machine Systems*, vol. 47, no. 4, pp. 462–473, 2017.

[18] D. Sieber, S. Musić, and S. Hirche, "Multi-robot manipulation controlled by a human with haptic feedback," in *IEEE/RSJ International Conference on Intelligent Robots and Systems*, 2015, pp. 2440–2446.

[19] S. Garrido-Jurado, R. Muñoz-Salinas, F. Madrid-Cuevas, and M. Marín-Jiménez, "Automatic generation and detection of highly reliable fiducial markers under occlusion," *Pattern Recognition*, vol. 47, no. 6, pp. 2280–2292, 2014.

[20] D. Honegger, L. Meier, P. Tanskanen, and M. Pollefeys, "An open source and open hardware embedded metric optical flow cmos camera for indoor and outdoor applications," in *IEEE International Conference on Robotics and Automation*, 2013, pp. 1736–1741.

[21] F. Farina, D. Fontanelli, A. Garulli, A. Giannitrapani, and D. Prattichizzo, "Walking ahead: The headed social force model," *PloS ONE*, vol. 12, no. 1, p. e0169734, 2017.